Dynamic phase separation in $La_{5/8-y}Pr_yCa_{3/8}MnO_3$

L. Ghivelder[1] and F. Parisi[2]
[1]*Instituto de Física, Universidade Federal do Rio de Janeiro, C.P. 68528, Rio de Janeiro, RJ 21941-972, Brazil*
[2]*Departamento de Física, Comisión Nacional de Energía Atómica, Av. Gral Paz 1499 (1650) San Martín, Buenos Aires, Argentina and Escuela de Ciencia y Tecnología, UNSAM, Alem 3901, San Martín, Buenos Aires, Argentina*
(Received 20 December 2004; published 31 May 2005)

Detailed magnetization measurements in $La_{5/8-y}Pr_yCa_{3/8}MnO_3$, including magnetic relaxation properties, demonstrate the dynamic nature of the phase separated state in manganites. The difference between the field-cooled-cooling and zero-field-cooled magnetization curves signals the existence in the latter of blocked metastable states separated by high energy barriers. Results of the magnetic viscosity show that the system becomes unblocked in a certain temperature window, where large relaxation rates are observed. We propose a simple phenomenological model in which the system evolves through a hierarchy of energy barriers, which separates the coexisting phases. The calculated magnetization curves using this model reproduce all the qualitative features of the experimental data. The overall results allowed us to construct an *H-T* phase diagram, where frozen and dynamic phase separation regions are clearly distinguished.

DOI: 10.1103/PhysRevB.71.184425 PACS number(s): 75.30.Kz

I. INTRODUCTION

The intense investigation of rare-earth perovskite manganites, triggered by the discovery of the well-known colossal magnetoresistance (CMR) effect, has revealed a variety of fascinating and intriguing physical properties.[1] Among these, the phenomenon known as phase separation (PS), the coexistence at different length scales of ferromagnetic (FM) metallic and antiferromagnetic (AFM) charge and orbital ordered insulating domains, has recently dominated the literature on manganese oxides, and is currently recognized as an intrinsic feature of several strongly correlated electron systems.[2] Among this class of compounds, $La_{5/8-y}Pr_yCa_{3/8}MnO_3$ is considered one of the prototype materials for the study of PS. The end members of the series, $La_{5/8}Ca_{3/8}MnO_3$ and $Pr_{5/8}Ca_{3/8}MnO_3$, have a robust low temperature FM metallic and charge ordered (CO) insulating states, respectively. The landmark paper by Uehara and co-workers,[3] using magnetic, transport, and electron microscopy techniques, showed evidence of two-phase coexistence for intermediate Pr contents. Additional investigations including NMR,[4,5] optical properties,[6] neutron scattering,[7] and a variety of complementing studies,[2] have corroborated the phase separation scenario. Nevertheless, a clear understanding of some basic macroscopic signatures of PS, including its dynamic behavior, is still lacking, and the true nature of the phase separated state is yet to be unveiled.

A relevant related issue deserving a great deal of attention nowadays is the glassy nature of the phase separated state.[8–11] The coexistence of FM and CO/AFM phases in manganites implies the frustration of different interactions, allowing the existence of glassy behavior. The key parameter for the formation of the glassy state is the introduction of some kind of controlled quenched disorder, which is able to open a window in the phase line separating FM and CO/AF phases.[12,13] Several experimental papers have reported glassy behavior in manganites,[14–16] which was attributed to cluster interaction within the phase separated state, rather than competition between double exchange and superexchange interactions.[9,10] Glass like dynamic effects such as aging and rejuvenation were also found in a phase separated manganite,[17] while a spin glass state with short range orbital ordering but without phase separation was observed in single crystals of $Eu_{0.5}Ba_{0.5}MnO_3$.[11] The spin dynamic of phase separated states is commonly superposed with the growth dynamic of one phase against the other.[17,18] Relaxation measurements performed on polycrystalline $La_{0.250}Pr_{0.375}Ca_{0.375}MnO_3$ revealed a high field mechanism related with the growth of the FM phase fraction, a process that was considered as arising from a new sort of magnetic glassiness.[19] Related effects such as cooling rate dependence on the transport and magnetic properties were also reported.[21,20]

In this paper we present a detailed study of the magnetic properties of polycrystalline $La_{5/8-y}Pr_yCa_{3/8}MnO_3$ [LPCM(y)], with emphasis on the $y=0.40$ sample. LPCM is one of the most studied phase separated systems,[22,23] and its (static) phase diagram as a function of y, temperature, and magnetic field was previously reported.[3,24] Here we focused our attention on the dynamic properties of the phase separated state. Due to large energy barriers and strains between the FM and CO-AFM states the system reaches low temperatures in a highly blocked metastable state. In this context, time relaxation measurements are important in order to reveal the equilibrium ground state. Our results showed the existence of a temperature window where large relaxation effects occur, and the relative fraction of the coexisting phases rapidly changes as a function of time. We have also performed calculations using a dynamical model, borrowed from creep theory of vortex dynamics,[25] which reproduces the main features of the experimental results. The model assumes a collective activated dynamics with divergingline functional form for the energy barriers. Interestingly, it predicts the existence of multiple blocked states in the phase separated regime, arising from the interplay between the temperature and the distance of the system to equilibrium; the existence of these blockade states was confirmed experimentally. Additionally, the results of magnetization as a func-

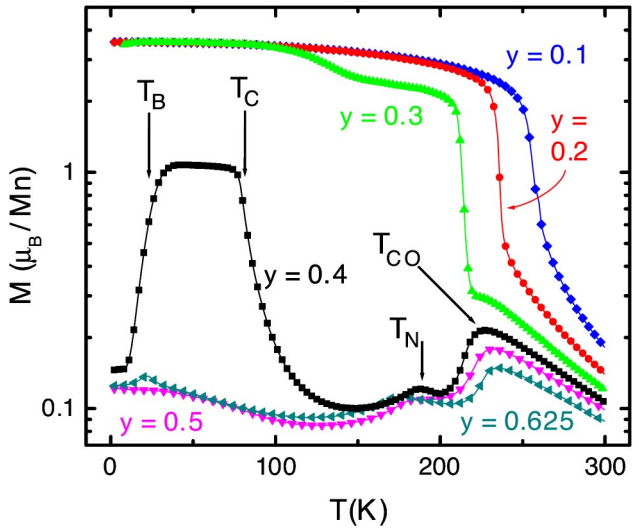

FIG. 1. (Color online) The temperature dependence of the zero-field-cooled magnetization of $La_{5/8-y}Pr_yCa_{3/8}MnO_3$, measured with $H=1$ T. For the $y=0.4$ sample the arrows indicate the charge-order transition temperature (T_{CO}), antiferromagnetic transition (T_N), ferromagnetic transition (T_C), and blocking temperature (T_B).

tion of temperature (T) and applied field (H) yield an H-T phase diagram of the compound, which reveals a boundary between dynamic and frozen phase separation effects.

II. EXPERIMENTAL DETAILS

The polycrystalline samples investigated were synthesized by the liquid-mix method starting from the metal citrates. After performing thermal treatments at 500 °C for 10 h and at 1400 °C for 16 h, the obtained powder was pressed into pellets and sintered for 2 h at 1400 °C. Scanning electron micrographs revealed a homogeneous distribution of grain sizes, of the order of 2 μm. A single crystal with Pr content $y\approx 0.375$ was also investigated. Magnetization measurements were performed with an extraction magnetometer (Quantum Design PPMS) as a function of temperature, applied magnetic field, and elapsed time. All temperature-dependent data was measured with a cooling and warming rate of 0.8 K/min.

III. EXPERIMENTAL RESULTS, DISCUSSION, AND PHENOMENOLOGICAL MODEL

In order to visualize the evolution of the magnetic properties as a function of the Pr content in the series, Fig. 1 shows the zero field-cooled magnetization of $La_{5/8-y}Pr_yCa_{3/8}MnO_3$ samples, measured with $H=1$ T. For low Pr contents ($y=0.1$ and 0.2), the behavior is similar to $La_{5/8}Ca_{3/8}MnO_3$, with a homogeneous FM state at low temperatures. The FM transition is shifted to lower temperatures for increasing Pr concentrations. The $y=0.3$ sample is also a nearly homogeneous ferromagnet at low temperatures, but the magnetization decreases through two steps when the temperature is increased. Phase separation occurs in this system at intermediate temperatures.[18,26] At the opposite end of the series, for high Pr contents ($y=0.5$ and 0.625) the magnetization curves display a peak at $T_{CO}\approx 230$ K, interpreted as arising from the CO transition,[27,28] and a shoulder at slightly lower temperatures, $T_N\approx 180$ K, identified through neutron data as arising from AFM order.[29] The low magnetization values indicate the existence of a negligible amount of FM phase at low temperatures. Within the phase diagram proposed by Dagotto and co-workers,[12,13] where the phase stability is governed by both temperature and an appropriate parameter g controlling interactions, the sample with $y=0.3$ is representative of the low g region, with a predominantly FM behavior at low temperatures, whereas the sample with $y=0.5$ displays features of the high g region. It is clear from the results plotted in Fig. 1 that the $y=0.4$ sample belongs to an intermediate region, where disorder induces a "glass" state in the system. The transitions at T_{CO} and T_N are still present, but the zero field-cooling magnetization show two additional features at lower temperatures, where phase separation phenomena are more pronounced. At very low temperatures the magnetization is characterized by low values; an estimation based on M vs. H data at 2 K yields a FM fraction of the order of 5%. As the temperature rises this FM fraction increases considerably at $T_B\approx 23$ K, a characteristic temperature indicated in the figure, and related to the unblocking of the low temperature frozen state,[30] as discussed in detail below. At $T_C\approx 80$ K this FM state becomes unstable, and the sample changes to the antiferromagnetic state.

We shall now investigate in more detail the behavior of the phase separated state below 100 K in the $y=0.4$ compound. Figure 2 shows the temperature dependence of the magnetization (a) and resistivity (b) of the LPCM(0.4) sample, measured with $H=1$ T using different experimental procedures: zero-field cooling (ZFC), field-cooled cooling (FCC), and field-cooled warming (FCW). Following the FCC curve in the magnetization data, a clear FM transition is observed at $T_C=45$ K, which is correlated with a metal-insulator transition in the resistivity plot. Below T_C the $M(T)$ curve changes quickly until $T\sim 25$ K. On further cooling no changes are observed in $M(T)$ down to the lowest temperature reached. As previously reported,[3–6,22,31] this compound behaves as phase separated below T_C, with coexistence between the CO-AFM and the FM phases. The magnetization value obtained at low temperatures, $M\sim 1\ \mu_B$/Mn, indicates that the FM fraction is around 30%.

However, the zero-field-cooled state of the sample is very different from this picture. The results of Fig. 2 show that after zero-field cooling the low temperature state of the system is insulating and has a very low magnetization value, suggesting that the sample is blocked in a metastable state with a predominance of the CO-AFM phase. Increasing the temperature in the presence of an applied field unblocks the system, promoting a growth of the FM phase over the AFM/CO one. The sample becomes metallic, and the magnetization reaches and even exceeds the values obtained in the FCC process. At higher temperatures the ZFC curve merges with the FCW one. The FCW curve coincides with that of the FCC data until a temperature around 25 K at which an increase of the magnetization (reaching values above those of the low temperature state) is observed; such effect is visible in several previous investigations.[22,31] This

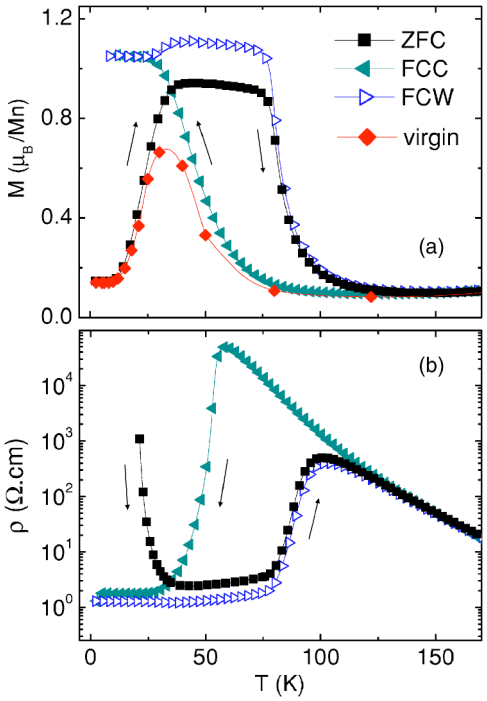

FIG. 2. (Color online) The magnetization (a) and resistivity (b) as a function of temperature of $La_{0.225}Pr_{0.40}Ca_{0.375}MnO_3$. Curves are measured with zero-field-cooled, field-cooled-cooling, and field-cooled-warming modes, with a field $H=1$ T. The procedure for obtaining the virgin magnetization curve is explained in the text.

fact is correlated with the decrease of the FCW resistivity curve above the reversibility temperature.

As a way to further investigate the magnetic behavior of the system we performed a novel experimental procedure to probe the magnetic response of the system, which we call *virgin* magnetization curve. In order to wipe out the effect of the magnetic field on the phase separated state, the sample is cooled without an applied field from room temperature, well within the paramagnetic state, to a certain target temperature, then the field is turned on to take a magnetization measurement, and subsequently the sample is again warmed to room temperature before proceeding to the next data point. Starting from higher temperatures, the results plotted in Fig. 2(a) show a magnetization rise arising from the FM transition, followed by a decrease due to the freezing of the higher temperature CO-AFM phase. The peak in the virgin magnetization curve coincides with the temperature where a change of behavior from metallic to insulating occurs in the FCC resistivity.

The relaxation phenomena were investigated by measuring the magnetization as a function of time, with $H=1$ T at various temperatures, after ZFC to the desired temperature. Selected results are show in a logarithmic scale the inset of Fig. 3. The $M(T,t)$ curves were adjusted with a logarithmic function

$$M(T,t) = S(T)\ln(t/t_0 + 1) + M_0(T) \qquad (1)$$

from which the magnetic viscosity S was extracted and plotted in the main panel of Fig. 3. At low temperatures the

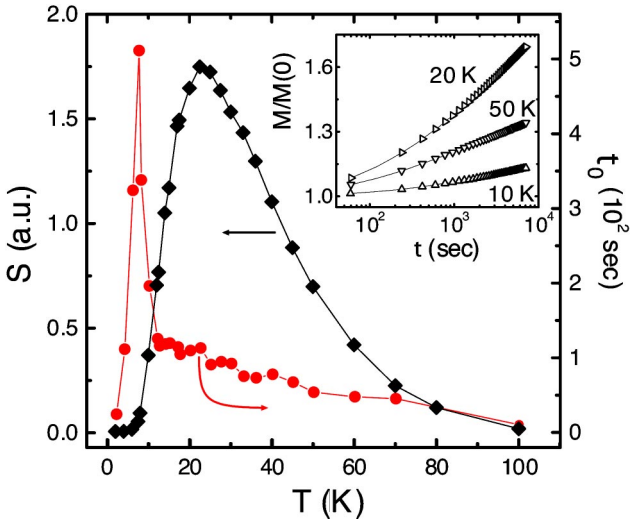

FIG. 3. (Color online) The temperature dependence of the magnetic viscosity S (left axis) and characteristic time t_0 (right axis) of $La_{0.225}Pr_{0.40}Ca_{0.375}MnO_3$, obtained by fitting the time dependence of the magnetization with Eq. (1). The inset shows the raw relaxation data, i.e., the time evolution of the normalized magnetization, after zero-field-cooling to selected temperatures, $T=10$, 20, and 50 K.

system is frozen in its phase separated state, in the sense that the (low) magnetization values measured do not evolve with time, i.e., $S(T)\approx 0$. As the target temperature is increased the thermal energy becomes high enough to allow the system to overcome the energy barriers between the coexisting phases. In this condition the FM phase fraction shows a substantial growth as a function of time, and the magnetic relaxation rate sharply increases. A peak in S is observed where the majority of the system becomes unblocked. At higher temperatures the FM fraction is closer to its equilibrium value, and S starts to decrease. The very large relaxation rates observed indicate that the description of the system based on a PS state is in fact a dynamic process, with the phase fraction of the coexisting states changing continuously as function of time in a certain temperature window. These relaxation measurements were also performed in a single crystal with similar Pr content, and the same results were obtained. This confirms that the dynamic effects observed are intrinsic to the material under investigation and not related to the granularity of the polycrystalline compound.

In Fig. 3 we have also plotted the temperature dependence of the macroscopic time t_0. This parameter can be interpreted as a measurement of the time scale at which the relaxation process occurs, taking into account that, within an activated picture of logarithmic relaxation, the height barriers U which can be overcome at time t are $U\approx T\ln(t/t_0)$.[25] The typical values obtained for t_0, around 10^2 s, are orders of magnitude larger than microscopic spin flip times ($\sim 10^{-12}$ s) and even larger than relaxation times of current densities in superconductors ($\sim 10^{-6}$ s) Interestingly, a sudden increase of t_0 is observed as T is lowered, showing a cusp around 7 K. This diverging like behavior resembles the conventional result of the standard theory of dynamic scaling near a phase transition,[32] indicating that a freezing process is happening.

To gain some additional insight into the low temperature behavior of the phase separated state we developed a simple phenomenological model, which reproduces the particular characteristics of the system. The main feature we wish to describe is the strong blocked state that develops at low temperatures, which is visible in both the ZFC and the FCC-FCW curves. The model has two basic assumptions: (*i*) the state of the system is collective; its evolution is described as a whole in terms of a single variable that represents the balance between the two phases, and (*ii*) its dynamic evolution is hierarchical, in the sense that the most probable event happens before the lesser probable one. Within this framework we propose a time evolution of the system through a hierarchy of energy barriers, which applies to the macroscopic parameters (the magnetization M or, equivalently, the ferromagnetic fraction x). The cooperative and hierarchical dynamics are present in the fact that the heights U of the barriers are dependent of the state of the system, i.e., $U=U(x)$. As x is a macroscopic parameter, such functional form implies that all the barriers (at the microscopic scale) of magnitude lower than $U(x)$ were overcome before the system reaches the state defined by the FM fraction x.

With these considerations, we propose a conventional activated dynamic functional form

$$\frac{dx}{dt} = \frac{(x_{eq} - x)}{|x_{eq} - x|} v_0 e^{-U(x)/T}, \tag{2}$$

where v_0 represent a fixed relaxation rate, and the prefactor gives the sign of the time evolution, depending whether the FM fraction is lower or higher than the equilibrium FM fraction, x_{eq}, at the given temperature and applied field. The dependence of the energy barriers with x is one of the main factors determining the dynamic characteristics of the system. To perform the calculations we chose a diverging energy barrier functional of the form $U(x)=U_0/|x_{eq}-x|$. In this way, the slow dynamic of the system as it approaches equilibrium is guaranteed. This kind of functional form applied for energy barriers has been extensively used to describe vortex dynamics in high T_C superconductors.[25] A simple linear form for $x_{eq}(T)$ was used, starting from $x_{eq}=0$ at $T_{start}=80$ K and ending with $x_{eq}=1$ at $T_{end}=2.5$ K. We used $U_0=134.4$ K, while the relaxation rate was set to $v_0=2\text{s}^{-1}$ Figure 4 shows the $x(T)$ curves obtained through the simulated FCC, FCW, and ZFC processes. A portion of the $x_{eq}(T)$ used is also displayed in the figure, in order to properly visualize the system behavior with respect to the equilibrium state. The FCC calculation was done starting at temperatures above T_{start} with an initial value x equal to zero. The temperature was lowered in steps of 0.5 K. At each stopping temperature a "measurement" was performed, which consists in waiting a measuring time $t_m=60$ S while the system is relaxing following Eq. (2). At the end of this time period, the value $x(T)$ was obtained, which in turn was the initial $x(T-0.5\ K)$ value for the next measurement. The FCW curve was acquired in a similar way, starting at T_{end} with an initial value $x(T_{end})$ equal to the last obtained in the FCC process. The ZFC curve was simulated starting with a low value of $x(T_{end})=0.02$. For completeness, we have calculated the *virgin* magnetization curve, starting at each temperature without a FM fraction, and performing the measurement at the end of a time $5t_m$, which is the estimated time to measure the $M(H)$ curve until $H=1$ T. The resulting curve (not shown) also reproduces very well the experimental results displayed in Fig. 2.

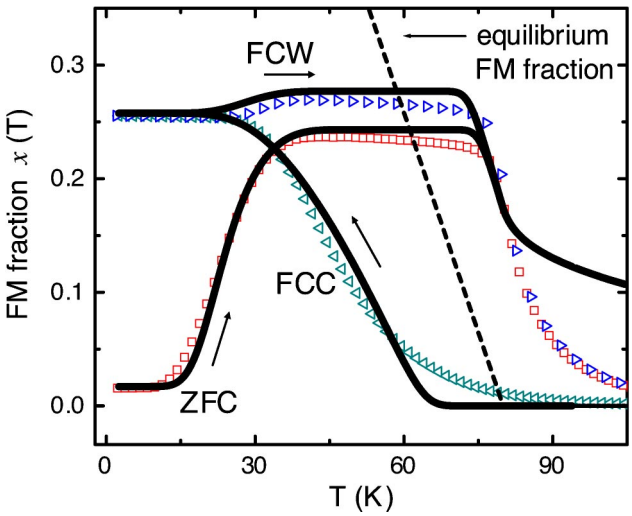

FIG. 4. (Color online) The ferromagnetic fraction obtained from magnetization data (symbols), compared to the calculated values (solid lines) using the model described in the text. The dotted line is the equilibrium ferromagnetic fraction, which reaches a value of 1.0 at low temperatures.

The qualitatively good agreement between the observed and calculated curves indicates that a collective mechanism is governing the dynamic evolution of the phase separated state. This very simple model reproduces several basic aspects of the physical response of the system, namely the existence of a strongly blocked state at low temperatures (visible in both the ZFC and in the FCC-FCW curves), the hysteresis observed in the whole process, the crossing between ZFC and FCC curves, and the increase of the FCC curve above the reversibility temperature. It is worth noting that the "reversible" behavior of the FCC-FCW curve at low temperature is a common feature of the manganites displaying phase separation, a singular fact not extensively discussed in the literature. In the above described framework it is clear that the reversible behavior is not the manifestation of an equilibrium state reached in the field cooling process, but the collective blockade of the system. When the temperature is high enough to unblock the system an increase of the magnetization in the FCW curve is observed. On further heating, $x(T)$ enters in a high temperature plateau that crosses the equilibrium curve, and gets into a regime with an excess of FM phase. Finally, at sufficiently high temperatures, the system enters a state characterized by the quick loss of its FM phase, although the complete FM to non-FM phase transition on heating cannot be fully reproduced, due to the fact that the model does not allow the system to reach the equilibrium state.

In addition, the dynamic model predicts the existence of multiple blockade regimes. This statement lies in the fact that the effective energy barriers distribution depends on both the

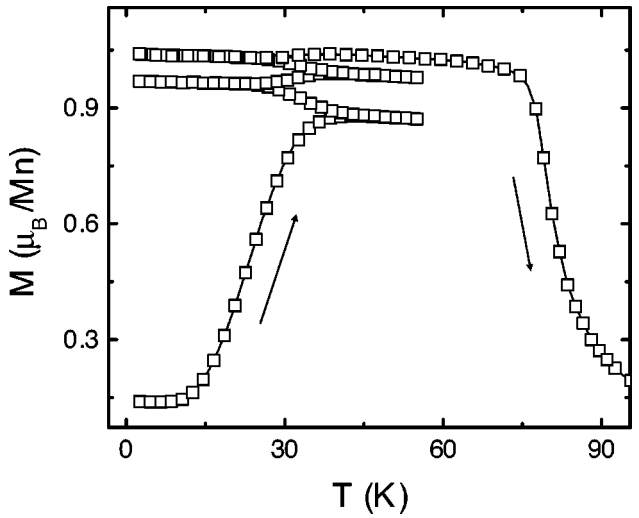

FIG. 5. The magnetization data, starting from zero-field-cooled data, with several cycles in the temperature window where large relaxation effects occur.

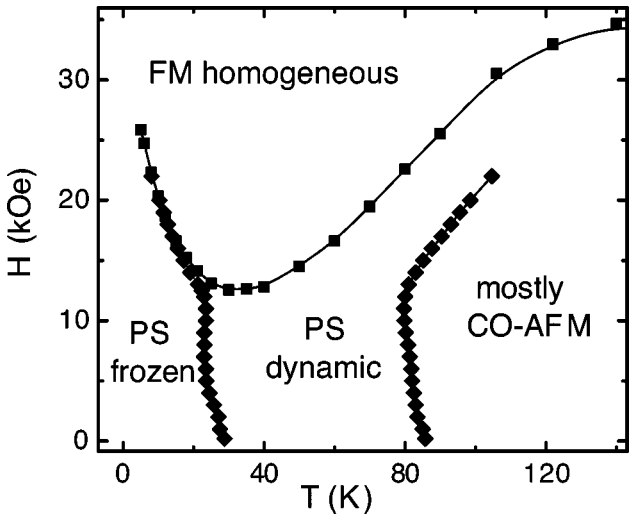

FIG. 6. The zero-field-cooled *H-T* phase diagram of $La_{0.225}Pr_{0.40}Ca_{0.375}MnO_3$., The lines represent phase boundaries obtained from *M* vs. *T* ($\diamond$) and *M* vs. *H* ($\square$) data, starting from the ZFC state. Hysteretic effects are not displayed. The regions depicted are homogeneous ferromagnetic at high fields, frozen phase separation at low temperatures, dynamic phase separation at intermediate temperatures, and mostly charge-order antiferromagnetic at higher temperatures.

temperature and the distance of the system to the equilibrium state. A crude estimation of a blocking condition can be made defining as blocked state that in which the FM fraction x changes less than the experimental resolution (around 10^{-5}) within the measuring time. For the model parameters used, these considerations lead to the condition

$$T|x_{eq} - x| \lesssim 8 \text{ K} \tag{3}$$

for the blocking regime of the system. It is readily implied that blocked states occur at low temperatures; within this framework the system is always blocked below 8 K, as experimentally observed. In addition, the relation is also satisfied in a temperature range where the FM fraction is close to its equilibrium value. This last condition is fulfilled at temperatures close to 60 K, where x reaches and eventually overcomes the equilibrium fraction (Fig. 4). For instance, through the functional form used for $x_{eq}(T)$, Eq. (3) implies that with a FM fraction $x=0.25$ the system will remain blocked in the temperature window between 45 K and 70 K. This feature is observed as a plateau in the calculated curves of Fig. 4. In order to test the validity of these ideas we have performed magnetization measurements under $H=1$ T on successive temperature cycles between 2 and 55 K. In this way states with different values of x are acceded. The obtained curve is shown in Fig. 5, where low and high temperature blocked states can be observed. These blocked states are characterized by the reversible behavior of the magnetization in the upwards and downwards runs. Both blocked regimes are separated by an unblocked region, which coincides with the temperature range with high relaxation rates (see Fig. 3). It is readily noticed that the temperature window in which the system is unblocked becomes narrow as the FM fraction increases with the number of cycles, as expected from Eq. (3).

The global results presented indicate that after zero-field cooling the sample reaches low temperatures in a highly blocked state, with a small and almost time-independent fraction of FM phase, which can be thought of as distributed in isolated regions or clusters surrounded by a CO matrix. This frozen-in state can be weakened and eventually destroyed by increasing the temperature at fixed magnetic fields or alternatively, by increasing the field at fixed temperatures. The latter leads to the well-known metamagnetic transition, where the entire system changes to a homogeneous FM state. Within this context, measurements of zero-field cooled *M* vs. *T* at various fields, and *M* vs. *H* at various temperatures enabled us to construct the *H-T* phase diagram of this prototype manganite compound. The results are shown in Fig. 6, where the different regions of the phase diagram are depicted. It is assumed that this phase diagram refers to the states reached after ZFC, i.e., it corresponds to the description of the system with low initial values of the FM fraction. At high fields, above the metamagnetic transition, the system is always in a homogeneous FM state. At low temperatures, as already mentioned, the system is frozen in a metastable configuration, where small FM regions are trapped in the CO-AFM background. As the temperature is increased there is a line in the phase diagram where the system becomes unblocked. Above this line the FM regions grow and became the majority phase in the phase separated state. In this region the magnetic relaxation rate is positive, and the phase separation can be viewed as dynamic phenomena, with the relative fraction of the coexisting states continuously changing with time. At temperatures even larger one crosses another line related with the FM transition. In this region the FM phase is no longer stable, and may exist solely as isolated clusters in the majority CO-AFM matrix.

IV. CONCLUSIONS

In summary, we performed an investigation of the low temperature magnetic properties in $La_{0.225}Pr_{0.40}Ca_{0.375}MnO_3$,

with emphasis on the dynamic behavior of the phase separated state. The slow logarithmic relaxation and the existence of field-dependent blocking temperatures are signatures that the phase separated state behaves, at least from a dynamic point of view, as a magnetic glass. The disorder induced by chemical substitution at the perovskite A site could be the cause of the "spread" of the free energy densities, giving rise to a complex landscape that can be comparable to the energy landscape in configurational space of true spin glasses. Our experimental data show that the dynamic of the system is better determined by the phase competition rather than by solely magnetic interactions as in conventional spin glasses. Such slow dynamic of the phase separated state is the main factor determining the magnetic response of the system in different dc experiments, and is at the basis of the well documented cooling rate dependence of their physical response.[21,20] The fact that the evolution of the phase separated state involves structural degrees of freedom could be the reason for the large values of the characteristic time t_0 observed. The agreement between the measured magnetization curves and the calculation performed with a model of cooperative hierarchical dynamics with diverging barriers, and the existence of multiple blockade regimes, gives a promising starting point to further investigate the properties of this dynamic phase separated state.

ACKNOWLEDGMENTS

The authors wish to thank G. Leyva for sample preparation and P. Levy for helpful discussions. The single crystal investigated was kindly given by S-W. Cheong. This work was partially supported by CAPES. Additional funding came from CNPq, CONICET, and Fundación Antorchas.

[1] M. B. Salamon and M. Jaime, Rev. Mod. Phys. **73**, 583 (2001).
[2] E. Dagotto, T. Hotta, and A. Moreo, Phys. Rep. **344**, 1 (2001); E. Dagotto, *The Physics of Manganites and Related Compounds* (Springer-Verlag, New York, 2003), and references therein.
[3] M. Uehara, S. Mori, C. H. Chen and S.-W. Cheong, Nature (London) **399**, 560 (1999).
[4] A. Yakubovskii, K. Kumagai, Y. Furukawa, N. Babushkina, A. Taldenkov, A. Kaul, and O. Gorbenko, Phys. Rev. B **62**, 5337 (2000).
[5] A. Gerashenko, Y. Furukawa, K. Kumagai, S. Verkhovskii, K. Mikhalev, and A. Yakubovskii, Phys. Rev. B **67**, 184410 (2003).
[6] H. J. Lee, K. H. Kim, M. W. Kim, T. W. Noh, B. G. Kim, T. Y. Koo, S.-W. Cheong, Y. J. Wang, and X. Wei, Phys. Rev. B **65**, 115118 (2002).
[7] S. Mercone, V. Hardy, Ch. Martin, Ch. Simon, D. Saurel, and A. Brûlet, Phys. Rev. B **68**, 094422 (2003).
[8] E. Dagotto, J. Burgy, and A. Moreo, *Nanoscale Phase Separation in Collosal Magnetoresistance Materials: Lessons for the Cuprates?* (Springer-Verlag, New York, 2002).
[9] I. G. Deac, J. F. Mitchell, and P. Schiffer, Phys. Rev. B **63**, 172408 (2001).
[10] F. Rivadulla, M. A. López-Quintela, and J. Rivas, Phys. Rev. Lett. **93**, 167206 (2004).
[11] R. Mathieu, D. Akahoshi, A. Asamitsu, Y. Tomioka, and Y. Tokura, Phys. Rev. Lett. **93**, 227202 (2004).
[12] H. Aliaga, D. Magnoux, A. Moreo, D. Poilblanc, S. Yunoki, and E. Dagotto, Phys. Rev. B **68**, 104405 (2003).
[13] E. Dagotto, New J. Phys. **7**, 67 (2005).
[14] J. M. De Teresa, M. R. Ibarra, J. García, J. Blasco, C. Ritter, P. A. Algarabel, C. Marquina, and A. del Moral, Phys. Rev. Lett. **76**, 3392 (1996).
[15] R. S. Freitas, L. Ghivelder, F. Damay, F. Dias, and L. F. Cohen, Phys. Rev. B **64**, 144404 (2001).
[16] J. Dho, W. S. Kim, and N. H. Hur, Phys. Rev. Lett. **89**, 027202 (2002).
[17] P. Levy, F. Parisi, L. Granja, E. Indelicato, and G. Polla, Phys. Rev. Lett. **89**, 137001 (2002).
[18] P. Levy, F. Parisi, M. Quintero, L. Granja, J. Curiale, J. Sacanell, G. Leyva, G. Polla, R. S. Freitas, and L. Ghivelder, Phys. Rev. B **65**, 140401(R) (2002).
[19] I. G. Deac, S. V. Diaz, B. G. Kim, S.-W. Cheong, and P. Schiffer, Phys. Rev. B **65**, 174426 (2002).
[20] L. M. Fischer, A. V. Kalinov, I. F. Voloshin, N. A. Babushkina, D. I. Khomskii, Y. Zhang, and T. T. M. Palstra, Phys. Rev. B **70**, 212411 (2004).
[21] M. Uehara and S.-W. Cheong, Europhys. Lett. **52**, 674 (2000).
[22] K. H. Kim, M. Uehara, C. Hess, P. A. Sharma, and S.-W. Cheong, Phys. Rev. Lett. **84**, 2961 (2000).
[23] J. A. Collado, C. Frontera, J. L. García-Muñoz, C. Ritter, M. Brunelli, and M. A. G. Aranda, Chem. Mater. **15**, 167 (2003).
[24] A. Yakubovskii, K. Kumagai, Y. Furukawa, N. Babushkina, A. Taldenkov, A. Kaul, and O. Gorbenko, Phys. Rev. B **62**, 5337 (2000).
[25] G. Blatter, M V. Feigel'man, V. B. Geshkenbein, A. I. Larkin, and V. M. Vinokur, Rev. Mod. Phys. **66**(4), 1125 (1994).
[26] M. Quintero, A. G. Leyva, P. Levy, F. Parisi, O. Agüero, I. Torriani, M. G. das Virgens, and L. Ghivelder, Physica B **354**, 63 (2004).
[27] H. Yoshizawa, H. Kawano, Y. Tomioka, and Y. Tokura, Phys. Rev. B **52**, R13145 (1995).
[28] Y. Tomioka, A. Asamitsu, H. Kuwahara, Y. Moritomo, and Y. Tokura, Phys. Rev. B **53**, R1689 (1999).
[29] Z. Jirák, S. Krupicka, Z. Simsa, M. Dlouhá, and S. Vratislav, J. Magn. Magn. Mater. **53**, 153 (1985).
[30] L. Ghivelder, R. S. Freitas, M. G. das Virgens, M. A. Continentino, H. Martinho, L. Granja, M. Quintero, G. Leyva, P. Levy, and F. Parisi, Phys. Rev. B **69**, 214414 (2004).
[31] V. Podzorov, M. Uehara, M. E. Gershenson, T. Y. Koo, and S.-W. Cheong, Phys. Rev. B **61**, R3784 (2000).
[32] J. A. Mydosh, *Spin Glasses: An Experimental Introduction* (Taylor and Francis, London, 1993).